Journal of Alloys and Compounds 509 (2011) 2326–2333

Contents lists available at ScienceDirect

Journal of Alloys and Compounds

journal homepage: www.elsevier.com/locate/jallcom

Evolution of nano-Ag_3Sn particle formation on Cu–Sn intermetallic compounds of Sn3.5Ag0.5Cu composite solder/Cu during soldering

L.C. Tsao*

Department of Materials Engineering, National Pingtung University of Science & Technology, 1, Hseuhfu Road, Neipu, Pingtung 91201, Taiwan

ARTICLE INFO

Article history:
Received 6 June 2010
Received in revised form 2 November 2010
Accepted 2 November 2010
Available online 11 November 2010

Keywords:
Ag_3Sn
Sn3.5Ag0.5Cu
Cu_6Sn_5

ABSTRACT

A Sn3.5Ag0.5Cu–0.5nano-TiO_2 composite lead-free solder was prepared by adding 20 nm TiO_2 to Sn3.5Ag0.5Cu (wt.%) solder. This study investigates the morphology of the intermetallic compounds (IMCs) formed during the soldering reactions between Sn3.5Ag0.5Cu–0.5nano-TiO_2 solder and Cu substrates at various temperatures ranging from 250 to 325 °C. The Cu_6Sn_5 grains formed in all soldering below 300 °C were scallop-type, while those formed at both 300 °C and 325 °C were prism-type in the early stage of soldering (less than 30 min). Also, Cu_6Sn_5 grains that formed at both 300 °C and 325 °C changed from prism-type to scallop-type with increasing soldering time. It is quite interesting that the morphology of Cu_6Sn_5 grains affects absorption by nano-Ag_3Sn particles. Especially, the scallop-type Cu_6Sn_5 grains formed by the ripening process are likely to be "captured" by the large amount of nano-Ag_3Sn particles.

These nanoparticles apparently decrease the surface energy and hinder the growth of the Cu_6Sn_5 IMC layer. In addition, the grain size of the nano-Ag_3Sn compounds increased with increasing soldering temperature and time. All these results indicate that Gibbs absorption theory can be used to explain the formation of these nanoparticles and their effects on the surface energy of the IMCs.

1. Introduction

Sn–Ag–Cu (SAC) solder is one of the earliest commercially available lead-free solders and also the most attractive candidate for surface mount technologies, as it provides better mechanical properties than do eutectic Sn–Pb solders [1,2]. However, precipitate bulk intermetallic compounds (IMCs) such as Ag_3Sn and Cu_6Sn_5, which is dispersed in the solder matrix, will seriously weaken the mechanical performance of a solder joint, even leading to failure under stressed conditions in actual service [3]. Kim et al. suggested that the formation of bulk IMCs could be prohibited effectively by increasing the cooling rate of solders or lowering the Ag concentration in these alloys [4].

Recently, numerous studies have revealed that additions of nano-TiO_2 particles to lead-free solders provide marked improvements in microstructure and mechanical properties, and such composite solders have attracted considerable attention. Lin et al. [5,6] demonstrated that a small amount of nano-TiO_2 addition has the ability to reduce undercooling efficiently and suppress the formation of massive primary Ag_3Sn plates. Tsao and Chuag [7] reported that the addition of TiO_2 nanopowders into a Sn3.5Ag0.25Cu solder reduced the average size and spacing of Ag_3Sn particles significantly. Additionally, many studies have tried to strengthen the novel lead-free solders by the addition of Al, ZrO_2, SiC, and SWCNT nanopowders, respectively [8–14].

It is well known that the reliability of the solder joint is affected by the growth of IMCs at the solder/metallization interface during soldering and aging/service, which weakens the solder joints due to the brittle nature of the IMCs. Recently, it has been shown that during Ag-containing solder/Cu substrate soldering, Ag_3Sn particles can be found on the surface of interfacial IMCs [15,16]. These particles decrease the interfacial energy and suppress the growth of the IMCs layer. Shen and Chan reported that the ZrO_2 nanoparticles absorbed Zn atoms on their surfaces, thereby impeding them from gathering on the surfaces of the Ni–Zn IMC layers and giving excessive growth, which improved the reliability of solder joints significantly [17]. Recently, we found that a great number of nano-Ag_3Sn particles form on the Cu_6Sn_5 IMCs when the solders contain Ag_3Sn precipitate phase after a lead-free Sn3.5Ag0.5Cu (SAC) composite solder/Cu substrate interface reaction. Based on this finding, the present work studies the evolution of nano-Ag_3Sn particles on Cu–Sn IMCs at different soldering temperatures and soldering times.

2. Experimental

TiO_2 nanoparticle-reinforced composite solders were prepared via mechanically incorporating 0.5 wt.% of about 20 nm TiO_2 particles (Nanostructured & Amorphous Materials, USA) into the Sn3.5Ag0.5Cu solder (SAC, Shenmao Technology, Inc., Taiwan) paste with subsequent remelting in a vacuum furnace and casting into

* Tel.: +886 8 7703202x7560; fax: +886 8 7740552.
E-mail address: tlclung@mail.npust.edu.tw

0925-8388/$ – see front matter © 2010 Elsevier B.V. All rights reserved.
doi:10.1016/j.jallcom.2010.11.010

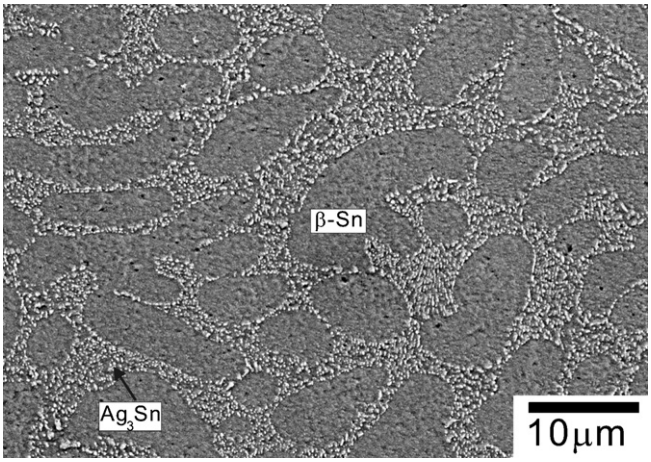

Fig. 1. The microstructure of the Sn3.5Ag0.5Cu composite solder.

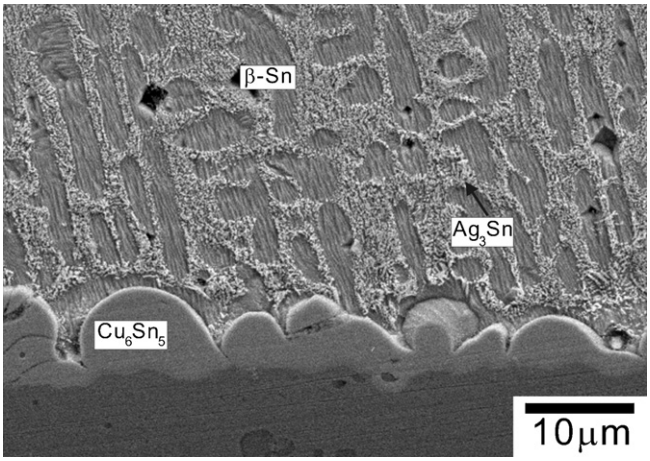

Fig. 2. The typical morphology of intermetallic compounds formed at Sn3.5Ag0.5Cu composite solder/Cu interfaces after soldering reaction at 250 for 60 min.

a mold. The solder was melted in a crucible and chill cast in a water-cooled copper mold to form square ingots of 8 mm × 10 mm × 20 mm. Then the solder was cold-rolled and a disk-type specimen (6 mm in diameter, 0.9 g) punched out. The 1 mm thick Cu substrate was polished with 1 μm and 0.3 μm Al_2O_3 powders, cleaned with acetone and alcohol, and coated with rosin mildly activated (RMA) type flux. For the study of interfacial reactions, the SAC–0.5nano-TiO_2 composite solder foil was placed on the Cu substrate and heated in a furnace under a vacuum of 10^{-3} Torr. Through a water cooling system installed within the furnace, the specimens were quickly cooled to room temperature. Soldering reactions were conducted at temperatures between 250 °C and 325 °C for various heating times ranging from 10 to 60 min.

In order to observe the morphologies of the IMCs, the unreacted solder covering the scallops was removed by mechanical polishing, followed by selective chemical etching. The selective etching solution was performed using 1 part nitric acid, 1 part acetic acid, and 4 parts glycerol. The morphologies were studied using a scanning electron microscope (SEM, s-3000H, Hitachi Co.) with a voltage of 20 keV. X-ray diffraction (XRD, D/max 2500 V/PC) and energy dispersive spectroscopy (EDS) were used to analyze the composition. For Ag_3Sn grain size analysis, the size of theAg_3Sn grains was calculated with the *Image-Pro* software and the average values calculated based on these data.

3. Results and discussion

The microstructure of the as-cast Sn3.5Ag0.5Cu composite solder is shown in Fig. 1; it contains dendritic β-Sn with a size of 10.6 μm, a small particle of Ag_3Sn, and a eutectic area where the Ag_3Sn phase is finely dispersed. The Ag_3Sn grains averaged 0.72 μm long and 0.44 μm diameter. However, large particles of Ag_3Sn and Cu_6Sn_5 were not observed in the rapidly cooled lead-free Sn3.5Ag0.5Cu composite solder. Fig. 2 shows the typical morphology of IMCs formed at Sn3.5Ag0.5Cu composite solder/Cu interfaces after soldering reaction at 250 °C for 60 min. It can be seen that a discontinuous scallop-shaped Cu_6Sn_5 layer had formed at the Sn3.5Ag0.5Cu composite solder/Cu interface after the soldering reaction. However, large particles of Ag_3Sn and Cu_6Sn_5 were not observed in the Sn3.5Ag0.5Cu composite matrix. In addition, a large number of dot-shaped submicro Ag_3Sn precipitates can be observed around the eutectic network structure. The XRD patterns of Cu_6Sn_5 layer that formed at the Sn3.5Ag0.5Cu composite solder/Cu interfaces reaction is shown in Fig. 3. The composite lead-free solders on top of the joints have been etched away with unreacted solder. The XRD pattern shows peaks of Cu_6Sn_5, Ag_3Sn and a low intensity of TiO_2. It is clear that the same crystalline Cu_6Sn_5 was formed at the interfacial layer between liquid Sn3.5Ag0.5Cu composite solders and Cu substrates heated at 250 °C for different soldering times. The crystal structure of the low temperature phase η-Cu_6Sn_5 is monoclinic [18]. However, different crystalline structures were observed in Cu_6Sn_5 grains at the interface between liquid Sn3.5Ag0.5Cu composite solders and Cu substrates soldered at 325 °C for 10 min. This indicates that the crystalline structure of the Cu_6Sn_5 grains was affected by the soldering temperature. In addition, a small intensity of nano-TiO_2 particles was also found. This means that aggregation of nano-TiO_2 particles may occur after reflowing.

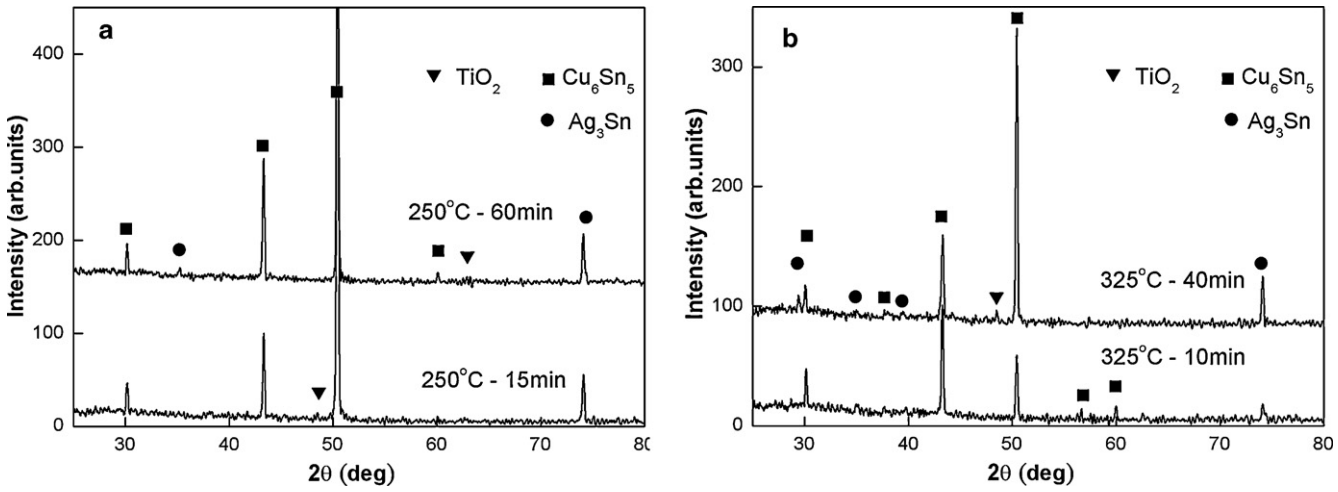

Fig. 3. XRD patterns of intermetallic compounds formed at Sn3.5Ag0.5Cu composite solders and Cu substrates soldering at different temperature: (a) 250 °C; (b) 325 °C.

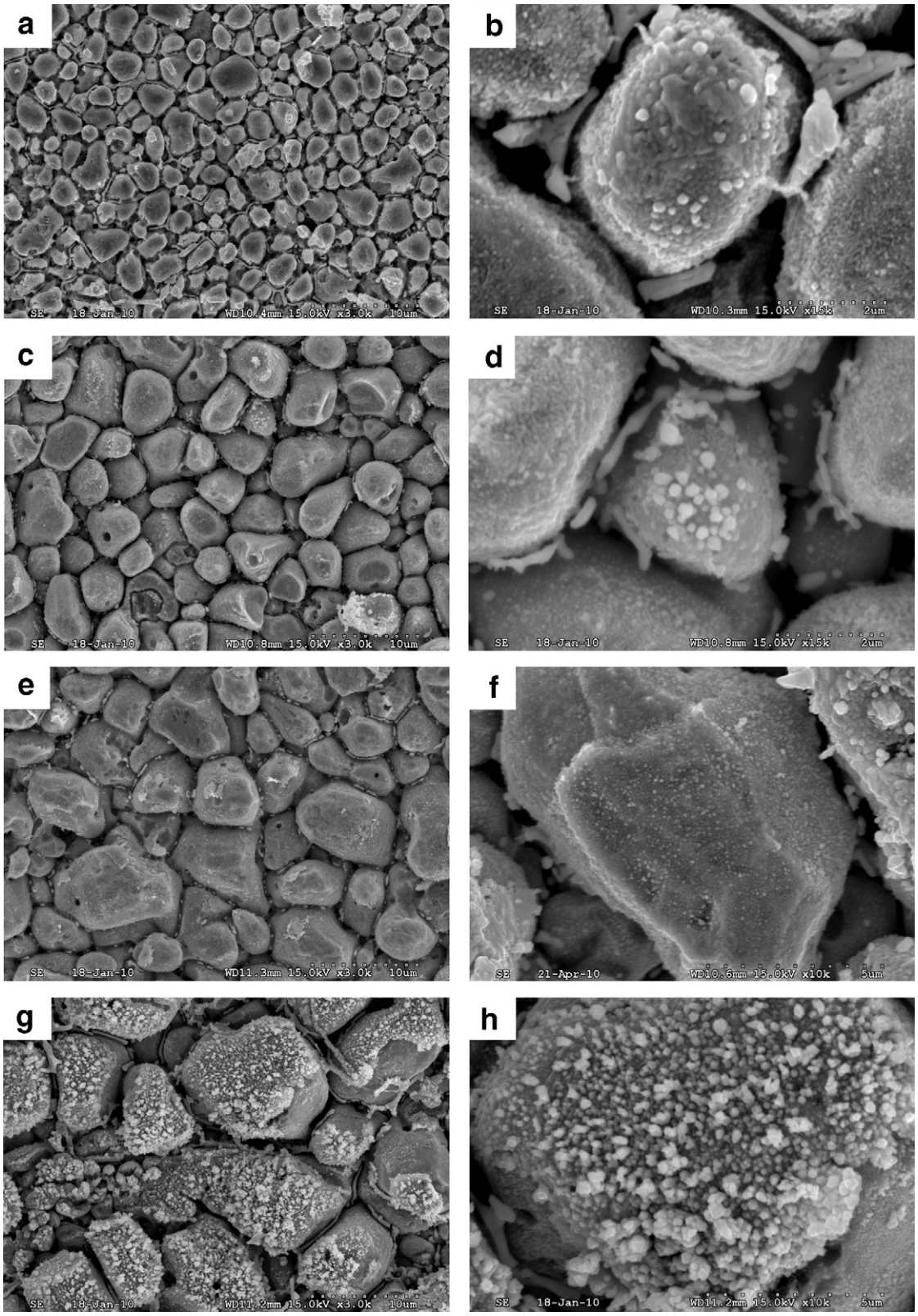

Fig. 4. The top views of Cu_6Sn_5 IMCs formed after the sample was soldered for 250 °C at different soldering times, followed by the solder being etched away: (a) 15 min; (b) (a) higher magnifications; (c) 30 min; (d) (c) higher magnifications; (e) 45 min; (f) (e) higher magnifications; (g) 60 min; (h) (g) higher magnifications.

The formation mechanism and reason will be discussed further below.

Fig. 4 shows the top surface morphology of the IMCs at the interface between liquid Sn3.5Ag0.5Cu composite solders and Cu substrates soldered at 250 °C for different soldering times. It is clear that scallop-type grains, Cu_6Sn_5 grains with a size of 3.3 μm, formed at the interface soldered for 15 min (Figs. 4a and b). These scallops appear rounded, and deep channels are visible between them.

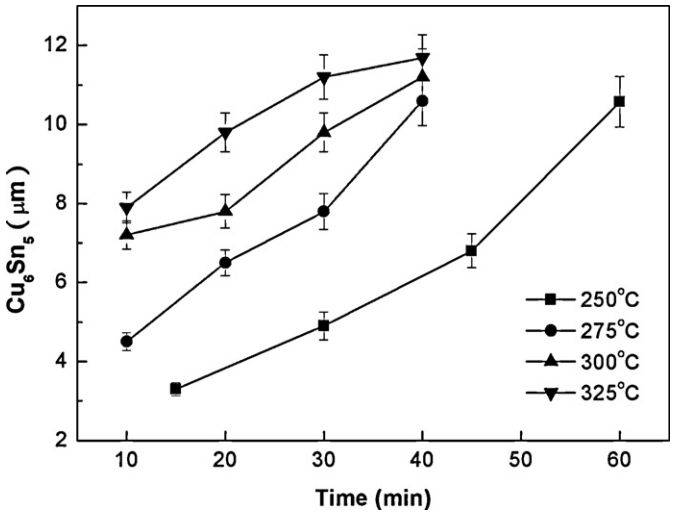

Fig. 5. The average sizes of Cu_6Sn_5 IMCs at different soldering temperatures.

The sizes of Cu_6Sn_5 grains after interfacial reaction between liquid Sn3.5Ag0.5Cu composite solder and Cu substrate at various temperatures for different soldering times are given in Table 1 and compared in Fig. 5. The Cu_6Sn_5 grains layer grew with an increase of reaction temperatures and time periods. In addition, the surfaces of the Cu_6Sn_5 grains at the Sn3.5Ag0.5Cu composite solder and Cu substrate reaction interface were rough, and light-colored particles were visible on the surface, as shown in Fig. 4a and b. According to the EDS analysis (Fig. 6), the scallop-type grains contained Cu, Sn, Ti, O and Ag. Since the solders used were SAC solder with nano-TiO_2 particles intermixed, and the Cu–Sn layer was the only phase at the interfacial between liquid Sn3.5Ag0.5Cu composite solders and Cu substrates, it can be concluded that these particles were composed of large amounts of nano-Ag_3Sn phase and trace amounts of TiO_2 nanoparticles. According to a previous study [19], the critical grain size at which the absorption behavior of Ag_3Sn particles on a Cu_6Sn_5 surface happens is about 2 μm. From SEM and XRD analysis, the lighted-colored nanoparticles were confirmed to be Ag_3Sn, which was adsorbed and filled in the surface of Cu_6Sn_5 grains soldered at 250 °C for different soldering times, as shown in Fig. 4. The Ag_3Sn nanoparticles with various sizes were visible on the surface of Cu_6Sn_5 IMCs. The reason is the unique properties of nano-TiO_2 particles. As active elements, nano-TiO_2 particles will accumulate

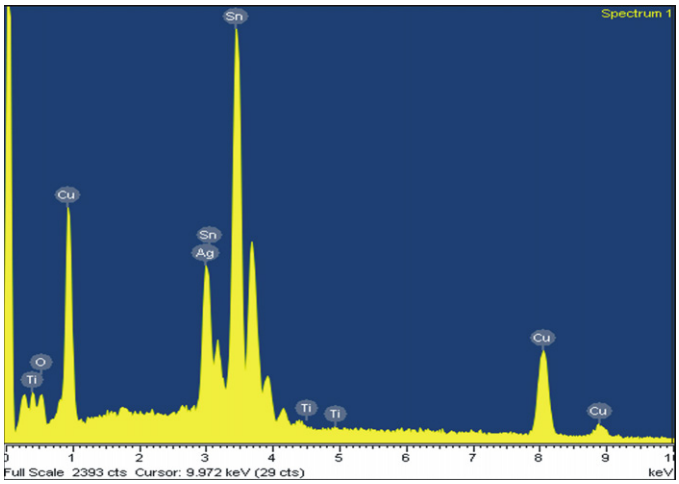

Fig. 6. EDS analysis to show the surface of the Cu_6Sn_5 grains.

at the interface of Ag_3Sn nanoparticles during both casting and reflowing. The average size of the nanoparticles was about 48 nm after heating at 250 °C for 15 min. With increased soldering time, the size of the nano-Ag_3Sn particles increased (Fig. 4c–h). It can be seen that a low intensity of TiO_2 peaks appears on the surface of Cu_6Sn_5 grains at long soldering times. This explains why some light-colored nanoparticles contain trace nano-TiO_2 particles.

In a recent study, Suh et al. [20] found that rooftop-type Cu_6Sn_5 grains that formed on (0 0 1) single crystal copper were elongated along two preferred orientation directions. In addition, Zou et al. [21] observed that regular prism-type Cu_6Sn_5 grains formed on (0 0 1) and (1 1 1) Cu single crystal substrate. The elongations aligned in two perpendicular directions. Furthermore, Cu_6Sn_5 grains changed from prism-type Cu_6Sn_5 grains to scallop-type after long soldering. This is similar to the morphology of Cu_6Sn_5 grains formed on Sn0.7Cu/Cu single crystal [22]. Fig. 7 shows the top views of Cu_6Sn_5 grains formed after the sample was soldered at 325 °C for different soldering times, followed by the solder being etched away. It is very interesting that the regular prism-type and scallop-type Cu_6Sn_5 grains formed at the interface between Sn3.5Ag0.5Cu composite solders and Cu substrate soldered at 325 °C for both 10–20 min and 30–40 min, respectively. This phenomenon was also observed in the 300 °C interface reaction. Comparing Figs. 4 and 7, the Cu_6Sn_5 grains in all soldering at 250 °C and 275 °C displayed common scallop-type Cu_6Sn_5, while those formed at both 300 °C and 325 °C displayed prism-type Cu_6Sn_5 in the early stage of the interfacial reaction (less than 30 min). From SEM and XRD analysis, we determined that the Cu_6Sn_5 grains that formed on Sn3.5Ag0.5Cu composite solder/Cu changed from prism-type to scallop-type with increasing soldering time. This formation of Cu_6Sn_5 grains with different shapes at the interface is difficult to explain. It is well known that more complex growth mechanisms govern the formation and morphological evolution of interface layers in the liquid tin–solid copper system, giving a scallop-type interface between the Cu_6Sn_5 and liquid tin. In the previous literature, Cui et al. observed that a scallop-type Cu_6Sn_5 layer formed on (0 0 1) single crystal Cu at 250 °C, but that a prism-type layer was generated at 300 °C [22]. Liu et al. reported that the compositions of IMC grains soldered for different times were the same, while the morphology changed from faceted to scallop-shaped [10]. Bian et al. [23] found that the presence of a medium-range order (MRO) structure in liquid metals is related to the content of the alloy composition, and closely related to the relevant phase structure in solid metals and temperature. In contrast, Zhao et al. have proposed that in liquid Sn0.7Cu, there is only a short-range order (SRO) structure, and its liquid structure is similar to that of pure Sn, while in Sn2Cu solder can be found not only SRO-Cu_6Sn_5 but also MRO-Cu_6Sn_5. The MRO-Cu_6Sn_5 clusters will form in liquid Sn2Cu solder. The MRO in liquid solder quickens the formation of interface IMCs in the very early stage of soldering and also accelerates the ripening process of IMC grains at the interface [19]. In our experiment, the Cu concentration of Sn3.5Ag0.5Cu composite solder was lower than that of Sn0.7Cu solder, so there may also have been SRO-Cu_6Sn_5 phase in the SAC composite solder. However, the Ag concentration of Sn3.5Ag0.5Cu composite solder is similar to that of eutectic Sn3.5Ag solder, and due to the higher affinity between Sn and Ag, there may be both SRO Ag_3Sn clusters and MRO Ag_3Sn clusters in liquid solder. Furthermore, the as-cast Sn3.5Ag0.5Cu composite solder had large amounts of nano-Ag_3Sn particles already. Thus, since the Cu concentration of the Sn3.5Ag0.5Cu composite solder was enhanced, there may be, in addition to SRO Cu_6Sn_5 clusters, MRO Cu_6Sn_5 clusters in liquid solder. This indicates that the MRO-Cu_6Sn_5 in liquid solder quickens formation of the scallop-Cu_6Sn_5 grains in the ripening process at the interface. As the content of Cu in Sn3.5Ag0.5Cu composite solder is lower than the solubility of Cu by about 2.65 wt.% at 300 °C [24], perhaps only prism-type Cu_6Sn_5 grains can form. Suh et al. [25]

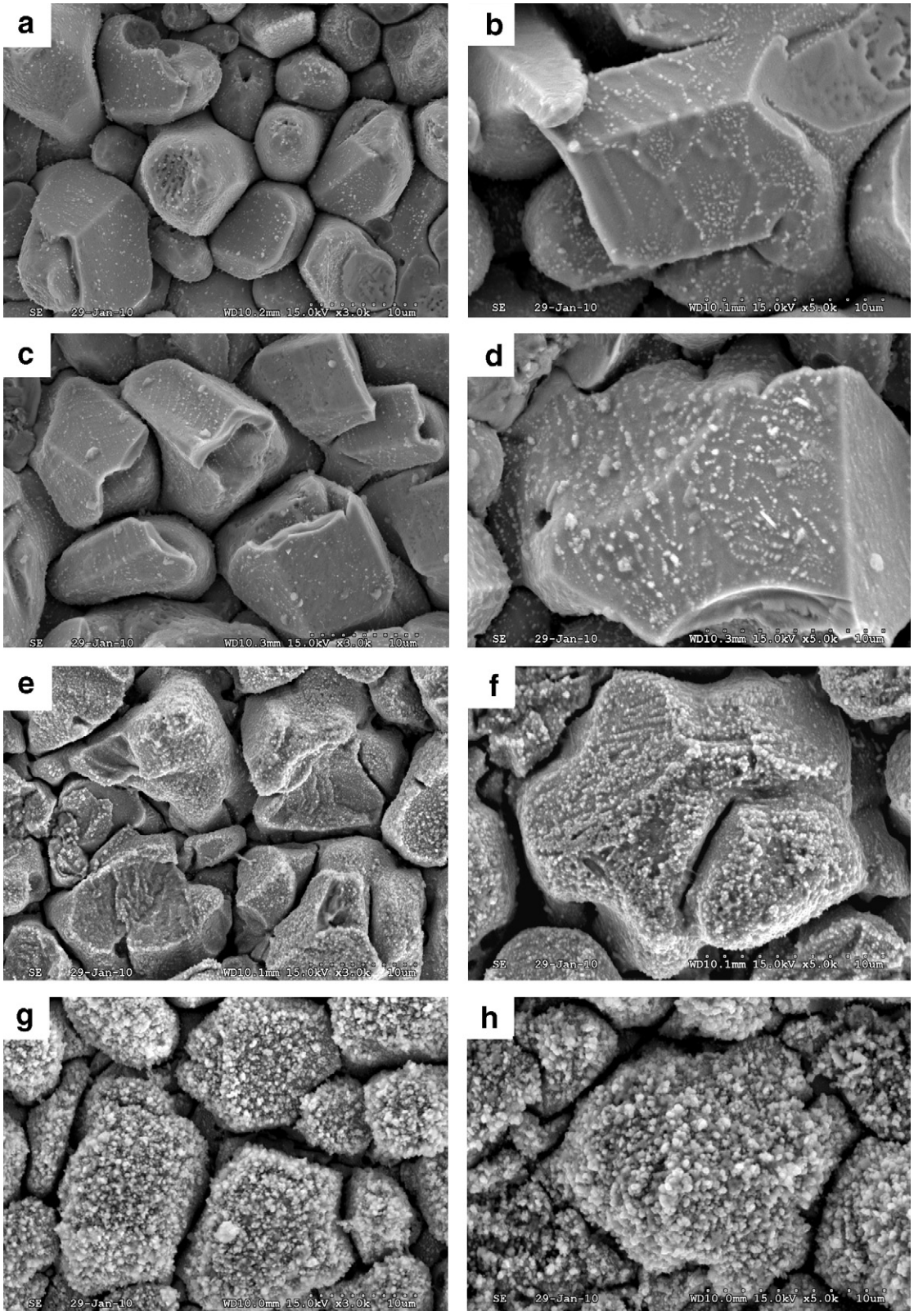

Fig. 7. The top views of Cu_6Sn_5 IMCs formed after the sample was soldered for 325 °C at different soldering times, followed by the solder being etched away: (a) 10 min; (b) 20 min; (c) 30 min; (d) 40 min. (a) 10 min; (b) (a) higher magnifications; (c) 20 min; (d) (c) higher magnifications; (e) 30 min; (f) (e) higher magnifications; (g) 40 min; (h) (g) higher magnifications.

found that the morphology of Cu_6Sn_5 was dependent on the composition of the solder. The scallop-type Cu_6Sn_5 became prism-type when the composition deviated further from the eutectic composition.

As shown in Fig. 7 and Table 1, the morphology of Cu_6Sn_5 grains formed on Sn3.5Ag0.5Cu composite solder/Cu changed from prism-type to scallop-type with increasing soldering time. As is well known, the Cu_6Sn_5 grains first form during the interfacial reac-

Table 1
Summary of observed scallop morphology and Ag_3Sn average size.

Reaction		Cu_6Sn_5			Ag_3Sn
Temperature (°C)	Time (min)	Morphology	Capture quantity	Grain size (μm)	Grain size (nm)
250	15	Scallop-type	Million	3.3	48
	30	Scallop-type	Million	4.9	75
	45	Scallop-type	Million	6.8	124
	60	Scallop-type	Million	10.6	250
275	10	Scallop-type	Million	4.5	64
	20	Scallop-type	Million	6.5	114
	30	Scallop-type	Million	7.8	175
	40	Scallop-type	Million	10.6	330
300	10	Prism-type	Thousand	7.2	172
	20	Prism-type	Thousand	7.8	243
	30	Prism-type	Thousand	9.8	312
	40	Scallop-type	Million	11.2	475
325	10	Prism-type	Thousand	7.9	220
	20	Prism-type	Thousand	9.8	280
	30	Scallop-type	Million	11.2	350
	40	Scallop-type	Million	11.7	493

tion between Sn-base solder and Cu substrate, and then another Cu_3Sn IMCs forms between the Cu_6Sn_5 layer and Cu substrate with increasing soldering time [26,27]. In this condition, the Cu atoms from the Cu substrate will react with the prism-type Cu_6Sn_5 to form the Cu_3Sn layer with longer soldering times. As a result, the nucleation of prism-type Cu_6Sn_5 grains will decrease with increasing soldering time, and the scallop-type grains will form [21]. This indicates that the morphologies of the Cu_6Sn_5 grains change with differences in soldering temperature and time. The morphology of Cu_6Sn_5 grains transformed at about 300 °C at the interface between Sn3.5Ag0.5Cu composite solders and Cu substrate soldering.

From the experiment, it is obvious that a small amount of nano-Ag_3Sn particles also formed, were adsorbed, and reticulated on the surface of prism-type Cu_6Sn_5 grains soldered at temperatures of both 300 °C and 325 °C for 10–20 min. However, it is quite clear that the great majority of the nano-Ag_3Sn particles were adsorbed and filled in the surface of Cu_6Sn_5 grains soldered at 300 °C and 325 °C for long times. This phenomenon is similar to the results of all soldering times at both 250 °C and 275 °C. However, this has not been observed in the recent literature [15,16]. This indicates that the morphology of Cu_6Sn_5 grains has a strong effect on nano-Ag_3Sn particle adsorption at the Sn3.5Ag0.5Cu composite solder/Cu interface after soldering. In these Sn-base solders, Sn, the main element, reacts with the substrate to form Sn–Cu or Sn–Ag IMCs layers. In addition, polycrystalline Cu substrate is currently widely used in electronics, and the scallop-type Cu_6Sn_5 grains grow larger but fewer with time, indicating that a ripening reaction occurs in Sn-base solder/Cu [19]. Meanwhile, the growth of the scallop-type Cu_6Sn_5 grain is supplied by two fluxes [21], the flux of the interfacial reaction and the flux of the ripening reaction, which indicates that the formation of Cu_6Sn_5 grains is accelerated by the higher Cu content in the liquid solder. The content of Cu in Sn3.5Ag0.5Cu composite solder is lower than the solubility of Cu in Sn, about 2.65 wt.% at 300 °C and 1.6 wt.% at 250 °C [25]. In the soldering reaction, Cu substrate was dissolved fast into the molten solder. The experimental data show that the ripening flux is dominant, about one order of magnitude greater than the interfacial reaction flux [19]. It is known that the greater the surface tension, the faster the plane growth, and the higher the adsorption quantity of surface-active materials [24]. Furthermore, it is reasonable to suppose that (1) the ripening process of the scallop-type Cu_6Sn_5 may be driving the nano-Ag_3Sn particle shifting near the IMCs; and (2) both the former nanoparticles and the new nano-Ag_3Sn precipitate are likely to be "captured" by the IMCs, which will decrease the surface energy of the scallop-type Cu_6Sn_5 grains and retard the growth of the whole IMC layer. However, the growth of the prism-type Cu_6Sn_5 grains is only supplied by the flux of the interfacial reaction. It is obvious that these nano-Ag_3Sn particles on the IMC surfaces are formed with a network (Fig. 7a–d). This indicates that these nano-Ag_3Sn particles were absorbed on the surface of prism-type IMCs, which takes place in the solidification process [15]. From SEM and XRD analysis, we know that the Cu_6Sn_5 grain morphology gradually transformed from a regular prism-type into a scallop-type at the longest soldering time, 30 min (Figs. 7e–h). The scallop-type Cu_6Sn_5 grains will quicken the absorption of a larger amount of active materials and decrease the interfacial energy. The above results indicate that the morphology of Cu_6Sn_5 IMCs greatly influences the absorption of nano-Ag_3Sn particles during the liquid-state interfacial reaction.

Liu et al. [16] reported that the effects of soldering time and temperature on the average size of Ag_3Sn particles are quite intricate. When soldering at the same temperature, the average sizes of nano-Ag_3Sn particles are almost the same with different soldering times. However, the nano-Ag_3Sn particles observed on IMCs were smaller at 300 °C than those at 250 °C, and those cooled in water were also smaller than those cooled in air. Yu et al. reported that the soldering time has little affect on the size of nano-Ag_3Sn particles [15]. They reported the formation of nano-Ag_3Sn particles and small amounts of Ag_3Sn particles on the surface of Cu_6Sn_5 grains in the solidification process. The average sizes of nano-Ag_3Sn particles on the surface of the Cu_6Sn_5 at different soldering temperatures and times are shown in Fig. 8 and Table 1. It is obvious that the grain size of nano-Ag_3Sn particles increased with increasing soldering temperature and times. This result is different from previous studies [15,16].

In a previous study, with the addition of a small percentage of nano-size particles to the eutectic solder, the more uniform precipitation of a large amount of nano-Ag_3Sn particles in the Sn3.5Ag0.5Cu composite solder has been obtained [28,29]. This phenomenon has also been found in this study. As effective surface-active materials, nano-TiO_2 particles will accumulate at the interface of nano-Ag_3Sn particles. It is well known that adsorption phenomena play an important role during solidification process of solder alloys and will greatly affect the microstructure. In addition, the absorption of nano-Ag_3Sn particles on the surface of Cu_6Sn_5 IMCs is analyzed. Thus, the theory of adsorption of surface-active materials can be used to explain its effect on the surface energy

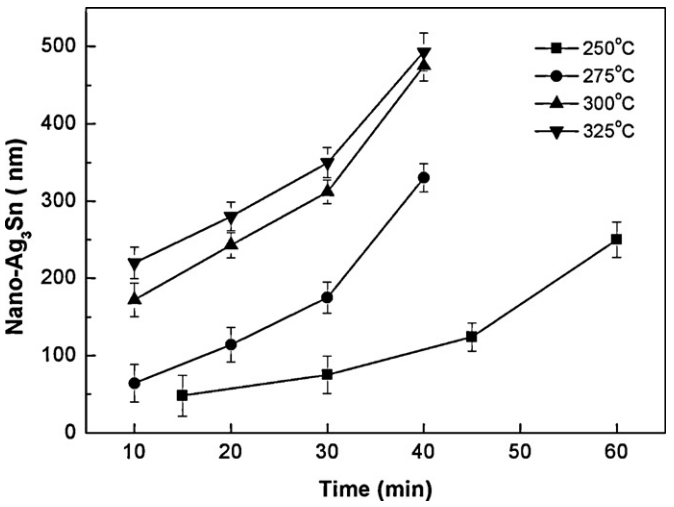

Fig. 8. The average sizes of nano-Ag_3Sn particles on the surface of the Cu_6Sn_5 at different soldering temperatures.

of Ag_3Sn and Cu_6Sn_5 IMCs, as nano-TiO_2 particles and nano-Ag_3Sn particles, respectively. Furthermore, this theory explains that the surface energy of the Cu_6Sn_5 grains decreased and suppressed the growth of the whole of the scallop-type Cu_6Sn_5 layer.

According to the Gibbs absorption equation [28–31], the adsorption amount of active material at the crystal plane K is

$$\Gamma^K = -\frac{C}{RT}\frac{\mathrm{d}\gamma^K}{\mathrm{d}C} \tag{1}$$

where Γ^K is the adsorption of surface-active material at crystal plane K, C is the total concentration of the active material, R is the Plank constant, T is the absolute temperature, and γ^K is the surface tension of the crystal plane K.

When crystal plane (Cu_6Sn_5 grain) K adsorbs a layer of active material (nano-Ag_3Sn particles), its surface tension can be deduced from the integral of the above equation (Eq. (1)).

$$\gamma_C^K = \gamma_0^K - RT\int_0^C \frac{\Gamma^K}{C}\mathrm{d}C \tag{2}$$

where γ_C^K is the surface tension of Cu_6Sn_5 grains K with adsorption of nano-Ag_3Sn particles, and γ_0^K is the surface tension of the Cu_6Sn_5 grains K without adsorption of nano-Ag_3Sn particles. Thus the surface free energy of the Cu_6Sn_5 grain is

$$\sum_K \gamma_C^K A_K = \sum_K \left(\gamma_0^K - RT\int_0^C \frac{\Gamma^K}{C}\mathrm{d}C\right)A_K \rightarrow \min \tag{3}$$

where A_K is the area of Cu_6Sn_5 grain K. Given that the volume is constant, the surface energy of the entire interface must be kept to a minimum in the equilibrium state. Here, $\sum_K \gamma_o^K A_K$ is assumed to be constant because it is independent of the concentration of nano-Ag_3Sn particles. That is,

$$\sum_K A_K \int_0^c \frac{\Gamma^K}{c}\mathrm{d}C \rightarrow \max \tag{4}$$

The relation indicates that the Cu_6Sn_5 grain with the maximum Γ^K value is most active. Therefore, this entire interface would capture the nano-Ag_3Sn particles preferentially; Gibbs tells us that the surface energy is reduced, and this reduction will decrease the growth velocity of this Cu_6Sn_5 grain. Until now, it has been quite difficult to calculate the surface energy in order to minimize the free energy of the entire interface in Sn3.5Ag0.5Cu composite solder/Cu substrate. Hence, there is no doubt that this plane will capture a large amount of the nano-Ag_3Sn particles formed on the scallop-type Cu_6Sn_5 IMCs layer, or several Ag_3Sn particles will be embedded on the prism-type Cu_6Sn_5 IMCs layer, which could reduce the interfacial energy during solidification. Moreover, the composite solder joints also were also effective in retarding the growth of the Cu_6Sn_5 IMC layer.

4. Conclusions

The reactions between Sn3.5Ag0.5Cu composite lead-free solder and Cu substrate at temperatures of 250–325 °C were investigated. The Cu_6Sn_5 grains that formed in all soldering below 300 °C displayed a common scallop-type morphology, while those formed at both 300 °C and 325 °C displayed a prism-type morphology in the early stage of soldering (less than 30 min). Furthermore, Cu_6Sn_5 grains that formed on Sn3.5Ag0.5Cu composite solder/Cu changed from a prism-type to a scallop-type morphology with increasing soldering time. Nano-Ag_3Sn particles were found on the surfaces of the Cu_6Sn_5 grains during the soldering process. It was found that the morphology of Cu_6Sn_5 grains affects the absorbed nano-Ag_3Sn particles. Especially, the scallop-type Cu_6Sn_5 grains that are formed by the ripening reaction are likely to be "captured" by the large amount of nano-Ag_3Sn particles. These nanoparticles decrease the surface energy and hinder the growth of the Cu_6Sn_5 IMCs. The grain size of the nano-Ag_3Sn particles increased with increasing soldering temperature and time. Absorption theory can be used to explain the formation of these nano-Ag_3Sn particles and their effects on the surface energy of the Cu_6Sn_5 IMCs.

Acknowledgments

The authors acknowledge the financial support of this work from the National Science Council of Taiwan R.O.C. under Project No. NSC97-2218-E-020-004.

References

[1] I. Anderson, J. Mater. Sci.: Mater. Electron. 18 (2007) 55–76.
[2] J. Glazer, J. Electron. Mater. 23 (1994) 693–700.
[3] K. Zeng, K.N. Tu, Mater. Sci. Eng. (R) 38 (2002) 55–105.
[4] K.S. Kim, S.H. Huh, K. Sugannuma, J. Alloys Compd. 352 (2003) 226–236.
[5] D.C. Lin, S. Liu, T.M. Guo, G.X. Wang, T.S. Srivatsan, M. Petraroli, Mater. Sci. Eng. A 360 (2003) 285–292.
[6] D.C. Lin, G.X. Wang, T.S. Srivatsana, M. Al-Hajri, M. Petraroli, Mater. Lett. 57 (2003) 3193–3198.
[7] L.C. Tsao, S.Y. Chuang, Mater. Des. 31 (2010) 990–993.
[8] J. Shen, Y.C. Liu, Y.J. Han, Y.M. Tian, H.X. Gao, J. Electron. Mater. 35 (2006) 1672–1679.
[9] J. Shen, Y.C. Liu, Y.J. Han, D.J. Wang, H.X. Tian, X. Gao, J. Mater. Sci. Technol. 22 (2006) 529–532.
[10] P. Liu, P. Yao, J. Liu, J. Electron. Mater. 37 (2008) 874–879.
[11] A.K. Gain, T. Fouzder, Y.C. Chan, A. Sharif, N.B. Wong, W.K.C. Yung, J. Alloys Compd. 506 (2010) 216–223.
[12] P. Babaghorbani, S.M.L. Nai, M. Gupta, J. Alloys Compd. 478 (2009) 458–461.
[13] X. Wang, Y.C. Liu, C. Wei, H.X. Gao, P. Jiang, L.M. Yu, J. Alloys Compd. 480 (2009) 662–665.
[14] K. Mohan Kumar, V. Kripesh, A.A.O. Tay, J. Alloys Compd. 450 (2009) 229–237.
[15] D.Q. Yu, L. Wang, C.M.L. Wu, C.M.T. Law, J. Alloys Compd. 389 (2005) 153–158.
[16] X.Y. Liu, M.L. Huang, Y.H. Zhao, C.M.L. Wu, L. Wan, J. Alloys Compd. 492 (2010) 433–438.
[17] J. Shen, Y.C. Chan, J. Alloys Compd. 477 (2009) 552–559.
[18] A.K. Larsson, L. Stenberg, S. Lidin, Z. Kristallogr. 210 (1995) 832–837.
[19] N. Zhao, X.M. Pan, H.T. Ma, C. Dong, S.H. Guo, W. Lu, L. Wang, Phys.: Conf. Ser. 98 (2008) 012029.
[20] J.O. Suh, K.N. Tu, N. Tamura, Appl. Phys. Lett. 91 (2007) 051907.
[21] H.F. Zou, H.J. Yang, Z.F. Zhang, Acta Mater. 56 (2008) 2649–2662.
[22] Y.P. Cui, M.L. Huang, 2009 International Conference on Electronic Packaging Technology & High Density Packaging (ICEPT-HDP 2009), 2009, pp. 593–596.
[23] X.F. Bian, X.M. Pan, X.B. Qin, M.H. Jiang, Sci. China 45 (2002) 113–119.
[24] M.L. Huang, T. Loeher, A. Ostmann, H. Reichl, Appl. Phys. Lett. 86 (2005) 181908.
[25] J.O. Suh, K.N. Tu, G.V. Lutsenko, A.M. Gusak, Acta Mater. 56 (2008) 1075–1083.

[26] Q.S. Zhu, Z.F. Zhang, J.K. Shang, Z.G. Wang, Mater. Sci. Eng. A 435–436 (2006) 588–594.
[27] T. Lauril, V. Vuorinen, J.K. Kivilahti, Mater. Sci. Eng. R 49 (2005) 1.
[28] L.C. Tsao, S.Y. Chang, C.I. Lee, W.H. Sun, C.H. Huang, Mater. Des. 31 (2010) 4831–4835.
[29] T.H. Chuang, M.W. Wu, S.Y. Chang, C.C. Ping, L.C. Tsao, J. Mater. Sci.: Mater. Electron., (2010) doi: 10.1007/s10854-010-0253-1, in press.
[30] Q.J. Zhai, S.K. Guan, Q.Y. Shang, Alloy Thermo-Mechanism: Theory and Application, Metallurgy Industry Press, Beijing, 1999, pp. 156–160.
[31] J. Shen, Y.C. Chen, J. Alloys Compd. 477 (2009) 909–914.